Combustion, obscurant and infrared emission characteristics of smoke composition based on red phosphorus and Mg-Al alloys

Pham Dinh Thang, Phan Duc Nhan, Nguyen Trung Toan*

Le Quy Don Technical University, No. 236 Hoang Quoc Viet, Cau Giay, Hanoi, Vietnam.
*Corresponding author: trungtoanktqs@mta.edu.vn
Received 13 Jul. 2024; Revised 8 Sep. 2024; Accepted 18 Sep. 2024; Published 14 Oct. 2024.
DOI: https://doi.org/10.54939/1859-1043.j.mst.IPE.2024.175-183

ABSTRACT

Infrared-obscurant formulations based on red phosphorus are widely utilized to protect military vehicles from laser and infrared guidance weapons. This work evaluates the influence of metal on the combustion, obscurant, and emission characteristics of red phosphorus-based smoke compositions. The research results demonstrated that the presence of Mg-Al alloy increased the combustion characteristics (such as combustion temperature, heat of combustion, burning rate, etc.) and infrared radiance in the wavelength range of 3 - 5 µm. However, this also reduces the 1.064 µm laser attenuation ability and the emission radiance in the wavelength range of 8 - 14 µm of the smokescreen compared to the metal-free composition. These findings provide insights into optimizing smoke composition, which has a high attenuation capability to 1.064 µm laser radiation and strong infrared emission in both wavelength ranges of 3 - 5 µm and 8 - 14 µm.

Keywords: Infrared emission; Obscurant; Smokescreen; Red phosphorus, Mg-Al alloy.

1. INTRODUCTION

In modern warfare, laser and infrared-guided weapons are commonly used to attack military targets such as tanks, warships, and fighter aircraft [1-6]. These combat vehicles have strong infrared emissions in the wavelength ranges of 3 - 5 µm (MIR - Mid-Infrared Band) and 8 - 14 µm (FIR - Far Infrared Band). As a result, smoke screens with concealing and decoying effects have been effectively developed as countermeasures to protect these combat vehicles. The smoke clouds were designed to attenuate laser radiation through absorption and scattering processes while simultaneously generating false thermal targets that were intended to attract and misdirect infrared-guided missiles [7-11].

In recent years, numerous obscurant formulations have been extensively researched, developed, and employed in military applications, including hexachloroethane (HC), white phosphorus (WP) mixtures, and compositions based on red phosphorus (RP) and nitrate salts [10, 12-14]. These compositions demonstrated excellent camouflage capabilities. However, they exhibited limitations in their spectral emission characteristics. Notably, the IR-screening smoke clouds generated from HC mixtures were mainly emitted in the 3-5 µm wavelength range, while those from RP and nitrate compositions were primarily active in the 8-14 µm range. Among various obscurant compositions, RP-based formulations have gained prominence in military applications due to their superior screening performance and lower toxicity than alternatives like WP or HC [13, 15, 16].

There are various methods to create a camouflage smoke screen, such as dispersing liquid mist or using pyrotechnic mixtures. Smoke compositions based on RP are mainly produced through the reaction of vaporized RP with oxygen in the air, which forms P_2O_5. Then, P_2O_5 interacts with moisture in the air, creating white smoke particles as a phosphoric acid aerosol with different levels of hydration [17, 18]. Recently, many scientists have been interested in improving and modifying smoke-producing mixtures based on RP. The goal is to ensure that the resulting smoke screens provide effective camouflage against laser radiation while emitting strongly in the 3-5 µm and 8-14 µm wavelength ranges [19-23]. Specifically, various metal powders and alloys were added to

the RP-based smoke composition to achieve the above objective. Cudzilo *et al.* [24] and Chen *et al.* [25] found that increasing the metallic content in Mg-Al/PTFE/Viton compositions leads to a higher combustion rate. Toan *et al.* [26] investigated the properties of IR-screening smoke, focusing on the impact of Mg-Al alloy powder characteristics, such as particle size and content, on combustion and infrared emission. Yi-kai Wang *et al.* [27] examined how different Mg/Al ratios in Al-Mg alloys affect the combustion characteristics of Al-Mg/PTFE infrared compositions. Toan *et al.* [28] also investigated the formulation and several characteristics of the smoke compositions based on RP. The components of the pyrotechnic smoke composition included RP (i.e., the primary component that generated smoke and reduced infrared radiation), sodium nitrate (i.e., an oxidizer that promoted the combustion process), Mg-Al alloy (i.e., provided energy and enhanced camouflage capability), polytetrafluoroethylene (PTFE, a fluorinated polymer that improved smoke properties), Viton A (i.e., a fluorinated rubber that created a homogeneous mixture), and manganese dioxide (i.e., a catalyst that enhanced combustion efficiency). Combining these components resulted in an effective smoke mixture, protecting military vehicles from guidance systems.

Currently, studies on the influence of metals on the combustion characteristics and infrared emission of RP-based mixtures continue to attract attention from scientists. However, it is noteworthy that limited scientific literature exists regarding the integration of Mg-Al alloy into RP-based mixtures, specifically addressing its implications on combustion processes, as well as obscurant and infrared emission characteristics. This study aims to evaluate how the presence of Mg-Al alloy affects the combustion characteristics (i.e., combustion temperature, ignition temperature, heat of combustion, burning rate), obscurant and infrared emission capabilities of mixtures based on Mg-Al and RP compared to the metal-free composition. The findings provide insights for developing improved obscurant formulations that offer balanced protection against laser and IR-guided threats.

2. MATERIALS AND METHODS

2.1. Materials

Table 1 presents the properties of the materials used in this paper, including abbreviation, mean particle size, purity, density, and manufacturer.

Table 1. *The properties of reagents.*

Reagents	Abbr.	Purity, %	Mean size, µm	Density, $g.cm^{-3}$	Source
Red phosphorus	RP	≥ 99	40	2.20	Shanghai Macklin Biochemical Co., Ltd
Magnesium-Aluminum Alloy	Mg-Al	≥ 98	50	1.90	
Teflon (PTFE)	$(C_2F_4)_n$	≥ 99	20	2.20	
Sodium nitrate	$NaNO_3$	≥ 98	60	2.25	
Manganese dioxide	MnO_2	≥ 85	10	5.03	
Viton A (66% F)	$C_{10}H_7F_{13}$	≥ 99	-	1.82	Dupont Company
Acetone	C_3H_6O	≥ 99.5	-	-	Xilong Co., Ltd.

Particle size distribution and scanning electron micrographs (SEM) of the main components, such as RP and Mg-Al alloy, are presented in Fig. 1.

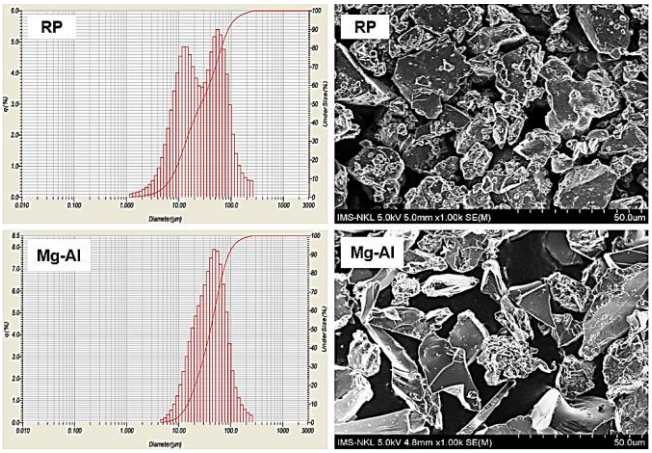

Figure 1. *Particle size distribution and SEM images of the main components.*

2.2. Experiment and methods

2.2.1. Sample preparation

The study proposes to assess the impact of metals on the characteristics of smoke mixtures by evaluating two RP-based formulations, one including and one excluding metals in their composition. The components of these samples are detailed in table 2.

Table 2. *The composition of samples.*

Samples	Content (wt.%)					
	RP	**Mg-Al alloy**	**PTFE**	**$NaNO_3$**	**MnO_2**	**Viton**
M0	75	-	10	6.5	0.5	8
M1	60	15	10	6.5	0.5	8

The sample preparation involved three stages: material preparation, component mixing, and granulation. Viton A rubber was dissolved in acetone at a 1:15 (w/v) ratio and left overnight. Precise amounts of powdered components were measured. The MnO_2 and $NaNO_3$ powders were combined, followed by PTFE and the Mg-Al alloy, and then stirred with the Viton solution. RP powder was added gradually, and then the mixture was sieved to 1.25 mm, air-dried, and vacuum-dried at 55 °C for 5 hours. The final mixture was packed in PE bags and stored in a desiccator. The ambient temperature and relative humidity during the mixing process were 30 °C and 65% RH, respectively.

2.2.2. Experimental techniques

The heat of combustion Q was determined using the Parr 6200 calorimeter (Parr Instrument Company, US). A 1.0 g sample was prepared for each measurement. Then, excess oxygen was pumped into the calorimeter bomb, and the combustion was ignited using an electrical igniter.

The ignition temperature was measured using the DT-400 (R&P, Germany) apparatus. The SP1 and SP2 temperatures were set to 150 °C and 350 °C, respectively. The heating rate SPr was set to 10 $K.min^{-1}$. The sample mass for each test was approximately 0.2 g.

The combustion temperature of RP-based compositions was measured using 50 μm thick WRe thermocouples. The samples were compressed in a 12 mm inner diameter, 25 mm high acrylic plastic tube with a compression force of 1 ton. The two halves of the sample surface were in direct contact with the thermocouple and had a conical shape. Measurements were taken at atmospheric pressure, and a graph of electromotive force versus time was obtained. This graph data was processed to convert it into temperature data. The experimental setup for measuring the combustion temperature using the thermocouple method is shown in Fig. 2.

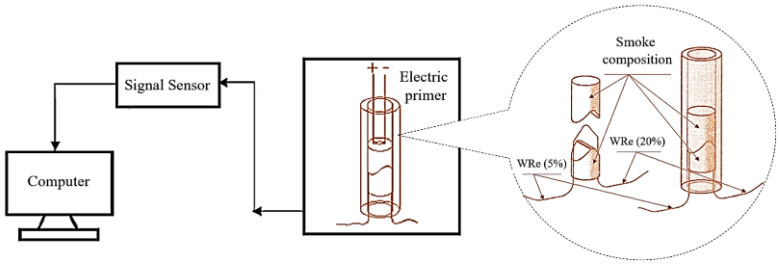

Figure 2. *Experimental setup for measuring the combustion temperature.*

To measure the burning rate, the RP–based samples were compressed into a cylindrical acrylic tube (25 mm in height, 12 mm in inner diameter) at different densities (1.0; 1.15; 1.30; 1.45; 1.60; 1.75) $g.cm^{-3}$ (Fig. 3a). Then, the compressed samples were carefully pushed out of the acrylic tube using a hydraulic compressor before being ignited (Fig. 3b). The sample was burned and observed in the open air, with the burning process recorded by a high-speed Fastcam SA 1.1 RV camera at 1000 fps (Fig. 3c). The ambient temperature and relative humidity during the test were 33 °C and 65% RH, respectively.

Figure 3. *Experimental setup for determining the burn rate*

The experimental setup for measuring the obscurant characteristics of 1.064 μm laser radiation is illustrated in Fig. 4. The degree of laser radiation attenuation was determined by comparing the initial laser power (without obscuring) with the laser power measured after passing through the screening smoke. A continuous-wave laser source with an output power of 11.0 mW and a beam diameter of 2.0 mm was directed through the cubical test chamber and measured by a laser power meter. The total path length through the screening smoke was 600 mm.

The transmittance T (i.e., the degree of transmission) was determined by:

$$T = \frac{I_{min}}{I_0} \quad (1)$$

where I_0 and I_{min} are the initial laser intensity without smoke and the minimum laser intensity after passing through the screening smoke, respectively.

The percentage attenuation (A) can be calculated using the following formula:

$$A(\%) = (1 - T).100 \quad (2)$$

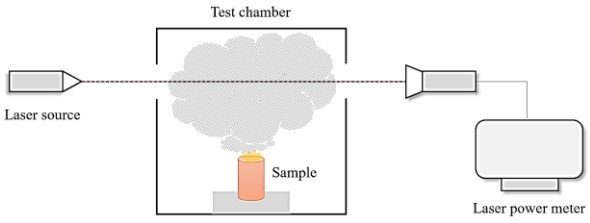

Figure 4. *Experimental setup for measuring the obscurant characteristics.*

Fig. 5 shows the experimental setup used to measure the infrared emission characteristics. The infrared radiation characteristics of smoke clouds were measured by the SR-5000N with a working wavelength from 2.5 - 14.0 µm. Ten grams of the sample were burned using an electric primer in a cubic test chamber with a volume of 0.216 m³. The lenses of the radiometer were positioned facing the smoke cloud through a source window on the wall of the test chamber, and the distance between the lenses and the source window was approximately 5.0 m. The emission intensity in the wavelength range from 2.5 to 14 µm was scanned every 2 seconds and repeated. The infrared emission intensity and radiance were determined using the built-in software.

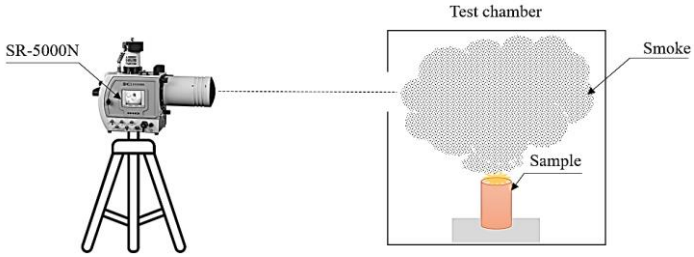

Figure 5. *Experimental setup for measuring the infrared emission characteristics.*

3. RESULTS AND DISCUSSION

3.1. Combustion characteristics

3.1.1. Combustion heat, ignition and burning temperature

The influence of Mg-Al alloy powder on combustion characteristics such as ignition temperature, combustion temperature, and heat of combustion for M0 and M1 samples is presented in table 3.

Table 3. *Combustion parameters of M0 and M1 samples.*

Samples	Ignition Temperature, (°C)	Burning Temperature, (K)	Heat of combustion, ($Kcal.kg^{-1}$)
M0	290	1018	4230
M1	301	1710	4525

Table 3 indicates that adding 15% Mg-Al alloy powder to the M1 sample improves its combustion characteristics by increasing its thermal reactivity. The presence of metals promotes a higher energy release due to more exothermic reactions, increasing the ignition and burning temperatures. This also results in a significantly higher heat of combustion for M1, reaching 4525 $kcal.kg^{-1}$, compared to 4230 $kcal.kg^{-1}$ in M0, indicating a more efficient energy and improved combustion performance.

The significant improvement in combustion characteristics of M1 compared to M0 can also be explained by the highly reactive nature of the Mg-Al alloy. This alloy creates a thermite reaction, releasing substantial heat and elevating the burning temperature. This leads to higher ignition and burning temperatures. Moreover, the oxidation reactions of the Mg-Al alloy contribute additional energy, significantly increasing the heat of combustion. As a result, the M1 sample exhibits superior combustion performance compared to the metal-free M0 sample.

3.1.2. Burning rate and combustion behavior

The average mass burning time and burning rate of M0 and M1 samples at different densities are shown in Fig. 6. As can be seen in Fig. 6, the presence of the Mg-Al alloy increases the average mass burning rate (i.e., decreases the burning time) of the M1 mixture compared to the M0 mixture at the same density. Moreover, increasing the compression density from 1.0-1.75 $g.cm^{-3}$ leads to a decrease in the burning rate (i.e., an increase in the burning time) for both M0 and M1 samples.

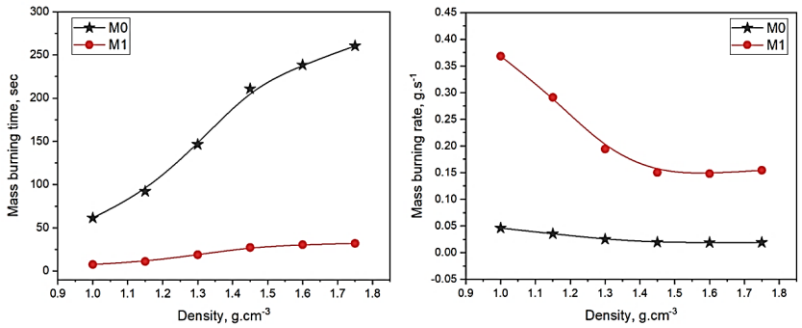

Figure 6. *Mass burning time and burning rate of samples at different densities.*

As noted by Toan [26], the reason is that increasing the compression decreases the spaces between the grains, which reduces the ability of hot gases to penetrate through the solid composition, consequently leading to a decrease in the average mass burning rate.

The combustion behavior and flame morphology of M0 and M1 at a compression density of 1.75 g.cm^{-3} are illustrated in Fig. 7.

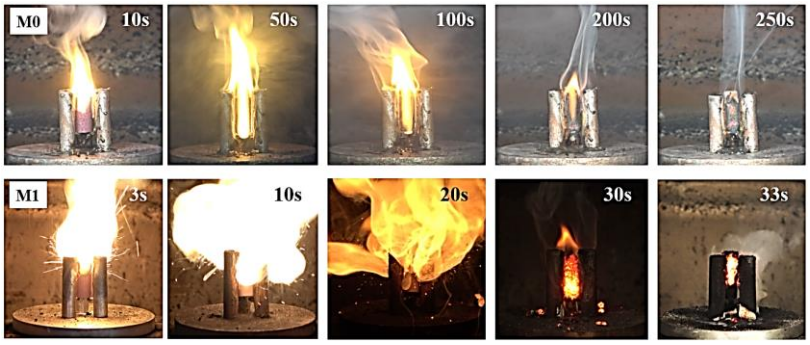

Figure 7. *Combustion behavior of M0 and M1 samples at a density of 1.75 g.cm^{-3}*

M0 displayed a weak flame, burnt for 7.5 times longer than M1, and produced excessive smoke, burning gradually while maintaining its shape. M1, containing 15% Mg-Al alloy, showed an intense flame, burned quickly in all directions, ejected molten products, produced less smoke than M0, and lost its original shape after burning. The presence of Mg-Al content accelerates and intensifies the combustion process, resulting in a shorter overall burning duration. This is due to the highly reactive nature of magnesium and aluminum, which can undergo rapid oxidation reactions when exposed to an oxidizing environment. Additionally, the Mg-Al alloy likely acts as a more efficient heat conductor, promoting faster ignition and flame front propagation by facilitating rapid thermal energy transfer.

3.2. Obscurant characteristics

The degree of laser radiation attenuation and the screening time for over 85% laser attenuation of M0 and M1 samples at different masses are illustrated in Fig. 8 and table 4. All samples were compressed to the same 1.75 g.cm^{-3} density in cylindrical acrylic tubes, similar to the burning rate measurement experiment described in section 3.1.2.

It is clear from Fig. 8 that the laser radiation attenuation capability of samples M0 and M1 increased significantly as the mass increased from 0.1 g to 1.1 g. This finding has direct relevance to practical applications, as it was attributed to more smoke being generated per unit of time with a larger sample mass, leading to more substantial laser radiation attenuation. At the same mass, M0 sample consistently exhibited a higher degree of attenuation and maintained attenuation above 85% for a longer time than M1. The main reason was the presence of Mg-Al alloy powder in M1, which reduced the content of the leading smoke-producing agent (RP) compared to M0 sample.

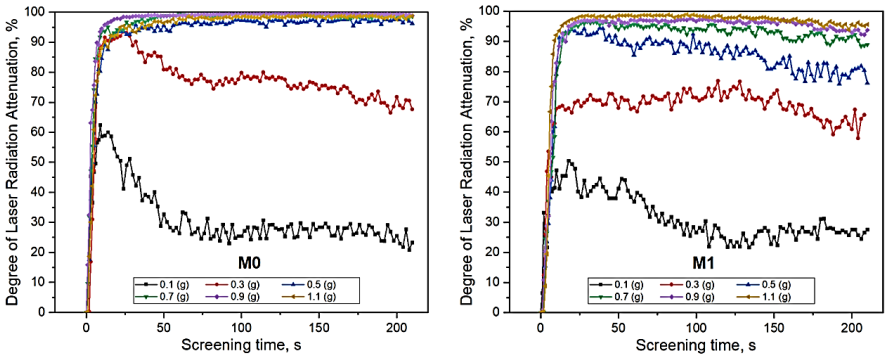

Figure 8. *The degree of laser radiation attenuation at different masses.*

Specifically, M0 contained 75% RP, while M1 contained only 60% RP, and 15% of the mass was replaced by Mg-Al alloy powder. This reduction in RP content was directly linked to a decrease in the smoke-generating ability of M1 sample.

Table 4. *Screening time for over 85% laser attenuation.*

Sample	Mass of samples, gram					
	0,1	**0,3**	**0,5**	**0,7**	**0,9**	**1,1**
M0	0 s	40 s	198 s	> 200 s	> 200 s	> 200 s
M1	0 s	0 s	128 s	> 200 s	> 200 s	> 200 s

Both samples exhibited excellent laser attenuation when the mass increased to 0.5 g. The duration of maintaining laser radiation attenuation above 85% for M0 and M1 samples was 198 seconds and 128 seconds, respectively. Furthermore, both samples exhibited laser radiation attenuation levels exceeding 85%, reaching nearly 100%, and screening time over 200 seconds at mass ranges from 0.7-1.1 g. This means that when the mass reaches 0.7 g, enough smoke is produced to obscure 85-100% of the incident's laser radiation.

The provided data suggest that the M1 sample, containing 15% Mg-Al alloy powder, exhibited a consistently lower degree of laser radiation attenuation compared to the M0 sample across all mass ranges. This reduced attenuation in the M1 sample implies that the addition of the alloy powder may have decreased the sample's capacity to absorb or scatter the incident laser energy.

3.3. Infrared emission characteristics

The average values of the infrared radiance of RP-based composition were measured using the SR-5000N Radiometer and the results are shown in table 5.

Table 5. *Infrared radiance of smoke clouds of the RP-based composition.*

Sample	Infrared radiance (10^{-2} W.sr^{-1}.cm^{-2})		Ratio of radiance in FIR/MIR band
	MIR band	**FIR band**	
M0	0.42	4.58	10.9
M1	2.84	3.71	1.3

The results in table 5 show that, along with the presence of Mg-Al alloy in the RP-based smoke composition, the infrared emission spectral distribution of smoke clouds changes significantly. In particular, while the smoke cloud of M0 formulation almost only emits infrared radiation in the wavelength of 8 - 14 μm (FIR), the smoke clouds of M1 emit infrared radiation in both the 3 - 5 μm (MIR) and 8 - 14 μm (FIR) bands.

This is explained by the fact that when using Mg-Al in the composition, the combustion characteristics (such as the combustion temperature, the heat of combustion, and the burn rate) of the M1 composition are higher than those of M0, leading to an increase in the radiation intensity in the MIR bands.

4. CONCLUSIONS

Both smoke compositions based on Red phosphorus have good laser energy attenuation properties. When using the M1 smoke composition, which contains Mg-Al, the burning characteristics such as ignition temperature, heat of combustion, combustion temperature, and burning rate are improved. However, the coverage capability of the smoke screen is slightly reduced compared to the M0 smoke composition. While the smoke clouds from the M0 mixture (i.e., metal-free) emit strongly only in the wavelength of 8-14 μm, the infrared spectral distribution of smoke clouds of M1 composition (with 15% Mg-Al alloy) appears in both 3-5 and 8-14 μm bands. Therefore, it is suggested that the smoke composition based on metal and red phosphorus could be used in smoke-generating equipment for the protection of warships or combat vehicles.

REFERENCES

[1]. Yang, L., et al., *"Analysis on the development of active protection system for tanks and armored vehicles"*. Journal of Physics: Conference Series.Vol. 1855, pp. 012034, (2021).

[2]. Suliman, H.M., et al., *"Anti-Tank Guided Missile System Design Based on an Object Detection Model and a Camera"*. International Journal of Computational Intelligence Systems.Vol. 16, pp. 16-20, (2023).

[3]. Titterton, D.H., *"Development of Infrared Countermeasure Technology and Systems"*, in Mid-infrared Semiconductor Optoelectronics. Springer London. (2006).

[4]. Krier, A., ed. , *"Mid-Infrared Semiconductor Optoelectronics"*. Springer. (2007).

[5]. Holst, G.C., et al., *"Modification of infrared signature of naval vessels"*. The International Society for Optical Engineering.Vol. 8355, pp. 518-528, (2012).

[6]. Milewski, S., et al., *"Coatings masking in near, medium, and far infrared used for ship camouflage"*. Electro-Optical and Infrared Systems: Technology and Applications VIII.Vol. 8185, pp. 269-278, (2011).

[7]. Mishra, K., *"Role of Smokes in Warfare"*. Defence Science Journal.Vol. 44, pp. 173-179, (2013).

[8]. Koch, E.-C., *"Metal Fluorocarbon Based Energetic Materials"*. John Wiley & Sons Ltd, Inc., West, pp. 197-209, (2012).

[9]. Smit, K., et al. *"Smoke Countermeasures for Army in the Visual and Infrared"*. 36th International Pyrotechnics Seminar. Rotterdam, The Netherlands (2009).

[10]. Stackleberg, K., et al., *"Military Smokes and Obscurants Fate and Effects: A Literature Review Relative to Threatened and Endangered Species"*. Construction Engineering Research Laboratory (U.S.). (2004).

[11]. Toan, N.T., et al., *"Obscurant and emission characteristics of the screening smoke composition used in naval ships"*. Journal of Military Science and Technology, pp. 108-117, (2020).

[12]. Greim, H., *"Hexachloroethane"*. Academic Press: Oxford. (2024).

[13]. Koch, E.-C., *"Special Materials in Pyrotechnics: V. Military Applications of Phosphorus and its Compounds"*. Propellants, Explosives, Pyrotechnics.Vol. 33, pp. 165-176, (2008).

[14]. Smith-Simon, C., et al., *"Toxicological profile for hexachloroethane"*. Research Triangle Institute, pp. 133-146, (1997).

[15]. Smit, K. *"Safety Related Aspects of Red Phosphorus Based Smoke Munitions"*. Proceedings of the 6th Australian Explosives Ordnance Symposium. Canberra, Australia (2003).

[16]. Cowden, J., *"IRIS Toxicological Review of Hexachloroethane (External Review Draft)"*. U.S. Environmental Protection Agency, Washington, DC, EPA/635/R-09/007A, pp. 5-72, (2010).

[17]. Klusáček, L., et al., *"The Use and Application of Red-Phosphorous Pyrotechnic Composition for camouflage in the infrared region of radiation"*. Propellants, Explosives, Pyrotechnics.Vol. 22, pp. 74-77, (1997).

[18]. Gautam, G., et al., *"Radiometric screening of red phosphorus smoke for its obscuration characteristics"*. Defence Science Journal.Vol. 56, pp. 377, (2006).

[19]. Li, J., et al., *"Burning and radiance properties of red phosphorus in Magnesium/PTFE/Viton (MTV)-based compositions"*. Infrared Physics & Technology.Vol. 85, pp. 109-113, (2017).

[20]. Cudziło, S., *"Studies of IR-Screening Smoke Clouds"*. Propellants, Explosives, Pyrotechnics.Vol. 26, pp. 12-16, (2001).

[21]. Suzuki, Y.M., K. & Suzuki, Y, *"IR-Screening properties of red phosphorus smoke"*. Kayaku Gakkaishi.Vol. 63(4), pp. 185-190, (2002).

[22]. Toan, N.T., et al., *"Obscurant and Radiation Characteristics of Infrared Screening Smoke Composition*

Based on Red Phosphorus". Defence Science Journal.Vol. 72, pp. 353-358, (2022).
[23]. Pulpea, B.G., et al., *"Design and Evaluation of Screening Smoke Compositions Based on Red Phosphorus in Open Field Conditions".* Applied Sciences.Vol. 12, pp. 12893, (2022).
[24]. Cudziło, S., et al., *"Studies of high energy composites containing polytetrafluoroethylene".* Archivum Combustionis.Vol. 20, pp. 59-71, (2000).
[25]. Chen, M., et al., *"The research on emission performance of Mg4Al3/PTFE infrared composition".* Laser and Infrared.Vol. 35, pp. 500, (2005).
[26]. Toan, N.T., et al., *"Effect of Mg-Al alloy powder on the combustion and the infrared emission characteristics of the Mg-Al/PTFE/Viton composition".* Defence Science Journal.Vol. 70, pp. 590-595, (2020).
[27]. Wang, Y.-k., et al., *"Effect of Mg-Al ratio on the combustion and infrared radiation properties of Al-Mg alloy/PTFE composition".* Journal of Physics: Conference Series.Vol. 2478, pp. 032023, (2023).
[28]. Nguyen, T.T., et al., *"Formulation and several characteristics of the smoke compositions based on red phosphorus".* Journal of Science and Technique-Section on Physics and Chemical Engineering. Vol. 2, pp. 120-130, (2024).

TÓM TẮT

Đặc trưng quá trình cháy, khả năng che phủ và phát xạ hồng ngoại của thuốc tạo khói trên cơ sở phốt pho đỏ và hợp kim Mg-Al

Thuốc hỏa thuật tạo khói trên cơ sở phốt pho đỏ (RP) được sử dụng nhằm bảo vệ các phương tiện quân sự trước các vũ khí dẫn đường bằng tia laze hoặc hồng ngoại. Bài báo này đánh giá ảnh hưởng của hợp kim Mg-Al đến đặc trưng cháy, khả năng che phủ và phát xạ hồng ngoại của thuốc hỏa thuật trên cơ sở phốt pho đỏ. Kết quả nghiên cứu chỉ ra rằng, sự có mặt của bột hợp kim Mg-Al trong thành phần làm tăng nhiệt lượng cháy, nhiệt độ bùng cháy và đặc biệt làm tăng khả năng phát xạ hồng ngoại của thuốc hỏa thuật trong dải bước sóng từ 3-5 µm. Tuy nhiên, việc thêm Mg-Al vào thành phần đồng thời làm giảm khả năng che phủ với tia laze có bước sóng 1.064 µm và khả năng phát xạ hồng ngoại trong dải bước sóng từ 8 - 14 µm của màn khói. Các kết quả nghiên cứu của bài báo bước đầu cung cấp các thông tin quan trọng nhằm tối ưu hóa thành phần khói có khả năng gây suy giảm bức xạ laze bước sóng 1.064 µm và phát xạ hồng ngoại mạnh trong cả hai dải bước sóng 3 - 5 µm và 8 - 14 µm.

Từ khóa: Phát xạ hồng ngoại; Che phủ; Màn khói; Phốt pho đỏ; Hợp kim Mg-Al.